Crystal implementation in SixTrack for proton beams

D. Mirarchi[*]*, S. Redaelli, W. Scandale*
CERN, European Organization for Nuclear Research, CH-1211 Geneva 23, Switzerland

Abstract

Crystal channeling is a property of crystals resulting from the extreme order in which the atoms are arranged: the crystalline lattice. Positive charged particles can get trapped between crystalline planes, and bending highly pure crystals allows deflecting high energy beams. Thus, they are very interesting for applications as primary collimator. The crystals installed in the Large Hadron Collider (LHC) provide a deflection that is equivalent to a magnetic field of about 300 T ideally acting only on halo particles. The implementation of a crystal routine in the framework of the collimation tools used at CERN for simulations of expected beam loss pattern around the entire machine (`SixTrack`) is therefore mandatory. The crystal routine presented here is suited for high statistics tracking simulations in large hadron accelerators. An introduction to the crystal physics relevant for our purposes is reported, on which the models implemented in the routine are based. Then, the implementation of these models in `SixTrack` is described.

Keywords
SixTrack; crystal; collimation.

1 Introduction

Coherent interactions in crystals are a very wide subject with many applications [1]. The main process of our interest is the planar channeling of positive charged particles. This allows to use efficiently bent crystals for the manipulation of hadron beams. In particular, the large deflection that can be given to channeled particles, makes crystals suitable for application as primary collimators. Moreover, the reduced nuclear interaction rate of particles trapped between crystalline planes with respect to particles traveling in amorphous materials, lead to a significant reduction of off-momentum losses around the accelerator [2].

The crystal routine presented here is based on a Monte-Carlo approach, so that interactions experienced when a particle traverses a crystal are randomly extracted from probability distributions as a function of the impact parameter. Particles are not tracked step by step inside the crystal volume but the various interactions possible are defined with a Monte-Carlo approach. This implementation was motivated by the need of a very fast routine that is suitable for high statistics simulations, i.e. about 10^7 protons tracked for thousands of turns in the accelerator. However, it can be considered as an emulation of the interactions that particles experience in a bent crystal, rather than a simulation that would involve solution of the equation of motion inside a crystalline potential. Although an approach based on first principles would allow simulations of a any crystalline structure, the time needed to solve the equation of motion would make complete loss map simulations unfeasible. Given the very high statistics and number of turns in the machine needed, an approach based on random extraction of interaction experienced from probability distributions was preferred. This is possible because all the known interactions that can occur in bent crystals are well described in the literature, and the few free parameters can be tuned using

[*]daniele.mirarchi@cern.ch

https://doi.org/10.23732/CYRCP-2018-002.91.

experimental data. It is also important to note that this routine, and what is reported later, is only valid for planar channeling of protons in silicon strip and quasi-mosaic bent crystals.

The tracking in the magnetic lattice of the machine is performed with `SixTrack` [3–6], which allows a symplectic, fully chromatic and 6D tracking, taking into account interactions with the ring collimators and the detailed aperture model of the entire machine. This code represents the standard tool used for accelerator physics studies at CERN, such as dynamic aperture and beam collimation. The complete benchmarking of the crystal routine and of its implementation in `SixTrack` are reported in [7, 8].

2 Crystal physics

At beginning of the twentieth century, physicists observed that a beam of charged particles can emerge from crystals, rather than be absorbed completely as happens in any other amorphous material of sufficient thickness. Driven by these observations Stark [9] made the hypothesis that in crystals an ordered internal structure is present. Thus, subsequent coherent interactions with such an ordered lattice can allow the particles to emerge from crystals. In amorphous materials the energy released by ionization as a result of the large number of random scatters leads to particle absorption. Only Si crystals are treated here, since they are the most suitable candidates to be used as particle deflectors, given their well developed manufacturing processes that lead to crystalline structures almost without imperfections [10, 11]. If this perfect crystalline structure is well oriented with respect to the incident particles, they will see it either as ordered planes or rows of atoms. Thus, particles can undergo coherent scattering and become trapped between planes (*planar channeling*) or on an axis (*axial channeling*). Given the higher efficiency of the planar channeling compared to the axial one, it is preferred for our applications. Moreover, planar channeling is preferred also because of easier operational manipulations needed to establish stable channeling. An additional degree of freedom would be needed to achieve the right orientation with respect to the beam envelope to channel particles between crystalline axis.

The theoretical approach reported in this paper is based on a classical treatment of interactions between particles and crystals, rather than using quantum mechanics. This is justified by two main reasons:

1. As shown in Section 2.1 particles trapped between crystalline planes oscillate in a harmonic potential. Therefore, their transverse energy is quantized and the number of energy levels is given by [12]:

$$n = \frac{d_p}{\hbar\sqrt{8}}\sqrt{U_{max} m\gamma}\,, \tag{1}$$

   where d_p is the distance between crystalline planes, U_{max} is the maximum of the potential well, and $m\gamma$ is the relativistic mass of the particle. Thus, if $n \gg 1$ it can be approximated as a continuous spectrum.
2. If the transverse de Broglie wavelength ($\lambda = h/p$, where p is the particle momentum) is much smaller than the channel width, the tunneling effect can be neglected.

At 120 GeV, the lowest energy of interest for collimation test purposes at CERN, one obtains: $n \sim 10^{13}$ and $\lambda \sim 10^{-17}$ m where $U_{max} \sim 20$ eV and $d_p = 1.92$ Å are used. Thus, the two conditions above are always fulfilled by ultra-relativistic particles.

2.1 Straight crystals

In order to derive a theoretical formulation of channeling phenomena, the potential between a particle and an atom is required. According to the Thomas-Fermi model the potential $(V(r))$ can be described as:

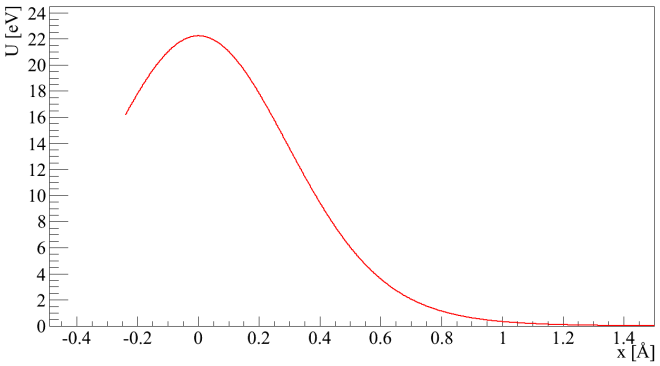

Fig. 1: Potential given by a single (110) silicon plane in the Molière approximation at room temperature.

$$V(r) = \frac{Z_i Z e^2}{r} \Phi(\frac{r}{a_{\mathrm{TF}}}) \,, \tag{2}$$

where $Z_i e$ is the charge of the impinging particle, Z is the atomic number of the target atom, r is the relative distance, and $\Phi(\frac{r}{a_{\mathrm{TF}}})$ is a Molière screening function that takes into account the electronic cloud around the nucleus [13]. Lindhard [14] asserts that: "under the hypothesis of small impact angle of the impinging particle with respect to the crystalline plane, we can consider the average potential generated from the entire crystalline plane as a continuous potential" given by:

$$U_p(x) = Nd \iint_{-\infty}^{+\infty} V(x,y,z) dy dz \,, \tag{3}$$

where x is the coordinate perpendicular to the crystal planes, N is the atomic density, d the distance from the plane and $V\,(x,y,z)$ is the potential in equation (2). Thermal agitation must also be taken into account. Considering this motion as independent of the location in the crystal and using a Gaussian spatial distribution for the atoms in the plane, the potential is given by the average over this distribution. The potential seen by a positive charged particle from an entire crystalline plane is illustrated in Fig.1.

Superimposing two planes, it is easily understandable that the potential (close to the minimum) seen by a particle between them will be a harmonic potential. This follows from the assumption that particles are influenced only by the potential of the closest planes; thus the entire potential well affecting the particle motion between crystalline planes can be approximated as:

$$U(x) \approx U_p(\frac{d_p}{2} - x) + U_p(\frac{d_p}{2} + x) \approx U_{max} \left(\frac{2x}{d_p}\right)^2 \,. \tag{4}$$

The outcome of exact calculation and the harmonic approximation of the potential above is shown in Fig. 2. A particle can be trapped between crystalline planes if its transverse momentum is lower than the maximum of the potential well. This implies the presence of a maximum impacting angle with respect to cristalline planes, the so called *critical channeling angle* (θ_c), below which channeling can occur. This angle depends on the particle momentum (pv) as [1]:

$$\theta_c = \sqrt{\frac{2U_{max}}{pv}} \,. \tag{5}$$

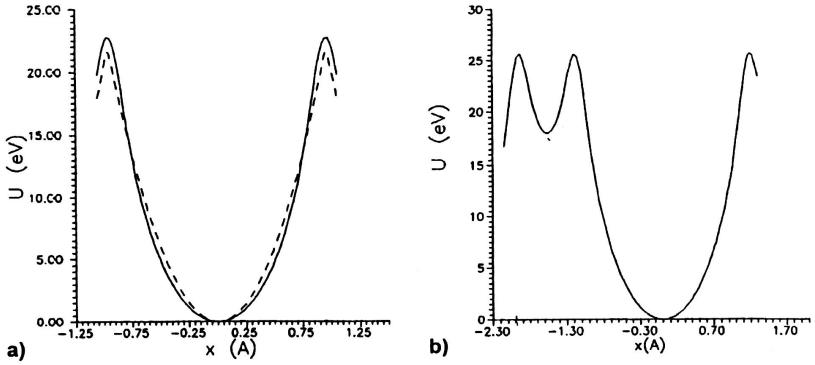

Fig. 2: Potential seen by a proton entering between crystalline planes at a small angle [1]. a) in silicon strip crystals where (110) planes are used, and with dashed line its harmonic approximation. b) in silicon quasi-mosaic crystals where (111) planes are used, with their characteristic ratio 1:3 of subsequent planes.

Using the harmonic approximation of the potential in which channeled particles are confined, they will follow a sinusoidal trajectory described by [1]:

$$x(z) = \frac{d_p}{2}\sqrt{\frac{E_t}{U_{max}}}\sin(\frac{2\pi z}{\lambda} + \phi)\,. \tag{6}$$

The oscillation phase ϕ is determined by the conditions at the entry of the crystal, and the oscillation period in the channel (λ) is given by:

$$\lambda = \pi d_p\sqrt{\frac{pv}{2U_{max}}}\,. \tag{7}$$

In conclusion, particles undergoing planar channeling will oscillate between crystalline planes, in a relatively empty space compared to what is present in an amorphous material. This is one of the most important features of crystals used in a particle accelerator to coherently steer particles for halo collimation purposes. It is worth introducing here the two main families of bent crystals: Strip (ST) and Quasi Mosaic (QM) crystals. In ST crystals the (110) planes are used to channel particles, while in QM crystals the (111) planes. The main difference is that the (110) planes are equidistant, whereas a ratio 1:3 is present in subsequent (111) planes, leading to the potential in Fig. 2 a) and b), respectively. This difference can be neglected in terms of channeling efficiency if protons are channeled, while it may become significant in case of channeling of heavy ions. The difference could be explained by the higher probability to experience nuclear interactions when heavy ions are trapped in the smaller channel of QM crystals.

2.2 Bent crystals

When a crystal is bent, the behavior of channeled particles does not differ significantly compared to what occurs in straight crystals. One can demonstrate that bent crystals can be simulated by adding a centrifugal force contribution to the potential of equation (4) [12]. Therefore, it is possible to define an effective potential as:

$$U_{eff}(x) = U(x) + \frac{pv}{R}x\,. \tag{8}$$

where pv/R is the term of centrifugal force in a crystal with bending radius R. The trajectory performed between crystalline planes is still sinusoidal, but ranges around a new equilibrium point due to the cen-

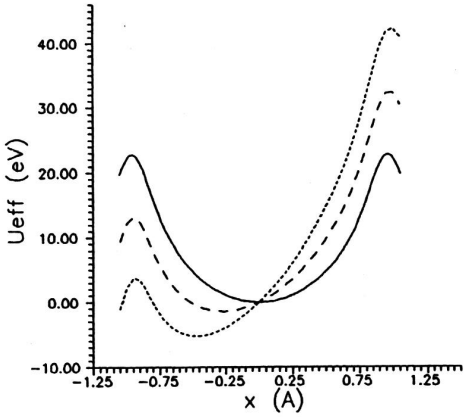

Fig. 3: Effective potential in bent strip silicon crystals [1]. Solid line refers to straight crystals, whereas dashed and dotted lines correspond to centrifugal forces of $\frac{pv}{R} = 1$ and 2 [GeV/cm], respectively.

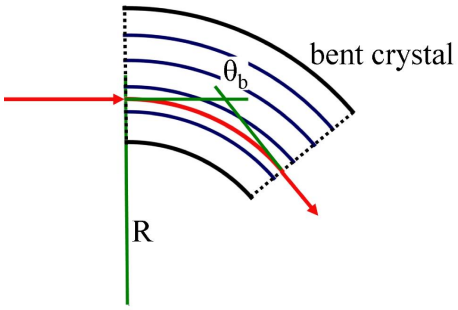

Fig. 4: Deflection given to particles channeled for the whole crystal length.

trifugal force. The dependence of this potential on the particle energy and the crystal bending radius is shown in Fig. 3. From this picture it is easy to infer the presence of a critical bending radius depending on the particle energy, after which the process of planar channeling is no longer possible, because of the insufficient depth of the potential well. The critical radius (R_c) can be understood as the radius for which the centrifugal force is equal to the maximum interplanar field. Thus the critical radius R_c for a given particle energy can be calculated from:

$$R_c = \frac{pv}{U'(x_{max})} \simeq \frac{pvx_{max}}{2U_{max}} , \tag{9}$$

where $U'(x_{max}) \approx 5\ \mathrm{GeV/m}$ in Si crystals [15], and is calculated in $x_{max} = d_p/2 - a_{TF}$ and not in $x = d_p/2$ because of the finite atomic charge distribution.

The new equilibrium point can be derived using the assumptions of equation (4) (but using now x_{max} instead of $d_p/2$) in the equation (8), which gives:

$$U_{eff}(x) = U_{max}\left(\frac{x}{x_{max}}\right)^2 + \frac{pv}{R}x . \tag{10}$$

Thus the minimum of the potential above will be at:

$$x_{min} = -\frac{pvx_{max}^2}{2RU_{max}} = -x_{max}\frac{R_c}{R} , \tag{11}$$

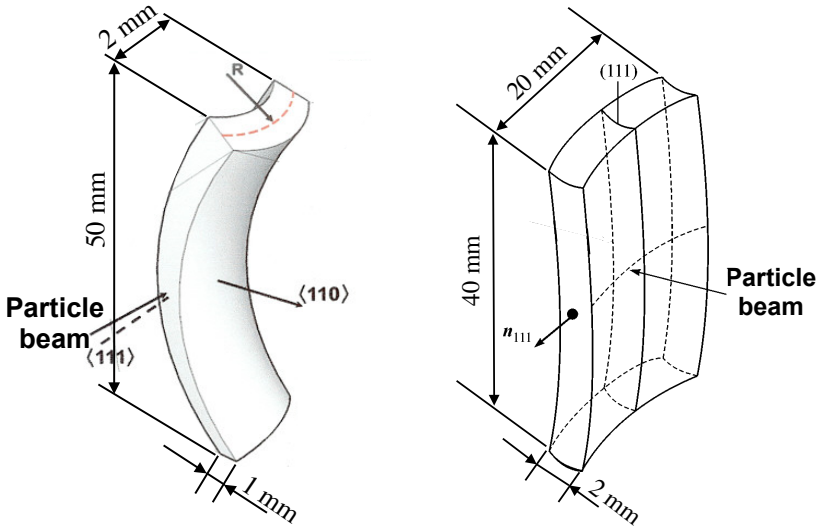

Fig. 5: Geometrical bending of a strip [10] (left) and a quasi-mosaic [16] (right) crystal, together with typical dimensions of crystals used for tests in the SPS.

In this condition, the reduced depth of the potential well[1] can be calculated as:

$$U^b_{max} = U_{eff}(x_{max}) - U_{eff}(x_{min}) = U_{max}\left(1 - \frac{R_c}{R}\right)^2 , \tag{12}$$

and the critical angle in a bent crystal is then:

$$\theta^b_c = \theta_c\left(1 - \frac{R_c}{R}\right) . \tag{13}$$

The equation of motion for particles channeled between bent crystalline planes can then be expressed as:

$$x = -x_{min} + x_{max}\sqrt{\frac{E_t}{U^b_{max}}}\sin\left(\frac{2\pi z}{\lambda} + \phi\right) , \tag{14}$$

which describes a sinusoidal trajectory, as in straight crystals, but oscillating around a new minimum x_{min}, with a different amplitude $\left(x_{max}\sqrt{E_t/U^b_{max}}\right)$, and same oscillation period λ. If the channeling regime is maintained for the whole length of the crystal, the channeled particle is deflected by an angle equal to the geometrical crystal bending:

$$\theta_b = \frac{l}{R} , \tag{15}$$

where l is the crystal length, as shown in Fig. 4. Obviously, this can only be achieved with pure crystals where the crystalline planes maintain a uniform bending along the whole crystal length, which is nowadays ensured by new bending techniques [10, 16]. An example of crystal bending in the case of ST and QM crystals is shown in Fig. 5, left and right respectively.

[1] i.e. the maximum transverse energy for which channeling is still possible.

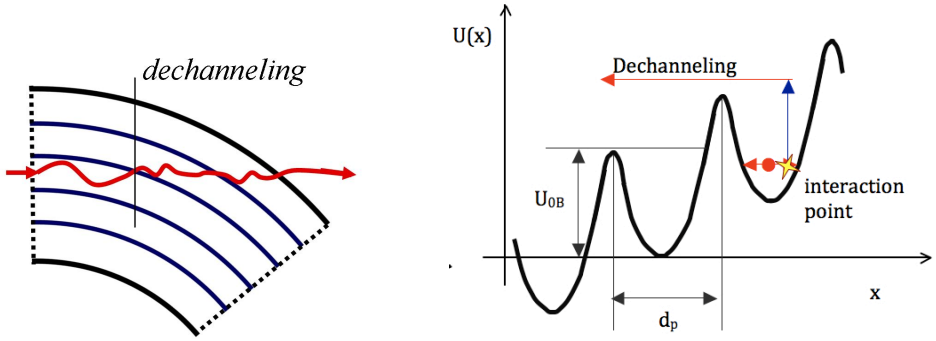

Fig. 6: Illustration of the dechanneling process.

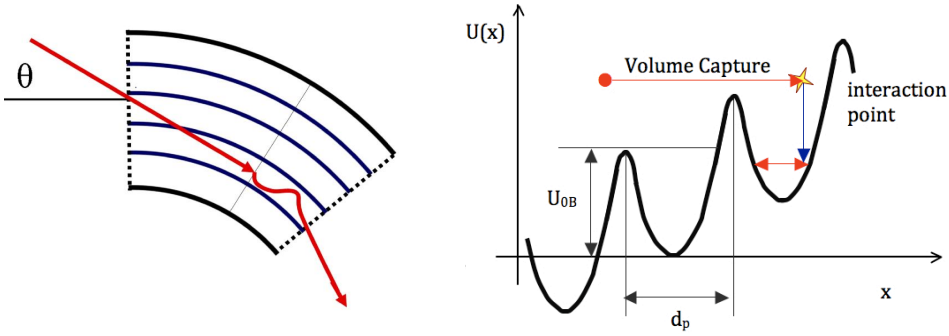

Fig. 7: Illustration of the Volume capture process.

2.3 Dechanneling and Volume Capture

When a particle is channeled between crystalline planes its transverse energy is not conserved, due to the scattering by electrons and nuclei. Channeled particles might therefore vary their transverse energy at each interaction, and can lose the condition for channeling if the interaction results in a total transverse energy above the maximum of the potential well. This condition is referred to as *dechanneling* (DC) and contributes to decrease the initial population of channeled particles, as shown in Fig. 6. On the other hand, a particle can enter the crystal structure with an energy slightly above the potential barrier. If the interaction results in a total transverse energy below the maximum of the potential well, a new energy state compatible with a bounded motion between crystalline planes can be achieved. This process is called *volume capture* (VC) and is shown in Fig. 7. Thus, the DC and VC processes can be considered as mutual to each other.

Let us now focus on the dechanneling process. As described above, channeled particles can increase their transverse momentum because of scattering from electrons in the channel, nuclei in the lattice or possible imperfections. Given the well established manufacturing process, the presence of imperfections can be neglected [11]. As discussed in [1, 12], the DC process can be described as an exponential decay of the initial population of channeled particles, which can be treated therefore as:

$$N(x) = N_0 \exp\left(-\frac{x}{L_D}\right) , \tag{16}$$

where N_0 is the initial number of particles that respect the channeling conditions at the crystal entrance, and $N(x)$ is the number of particles still in channeling after a path x in the channel, for a given *char-*

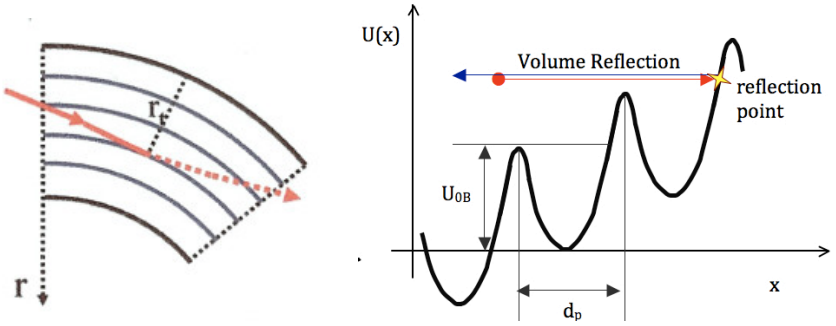

Fig. 8: Illustration of the volume reflection process.

acteristic dechanneling length (L_D). Using diffusion theory it is possible to derive the contribution given by interactions with electrons in the crystalline channel [1], leading to the *characteristic electronic dechanneling length*, which can be written as:

$$L_D^e = \frac{256}{9\pi^2} \frac{pv}{\ln(2m_e c^2 \gamma / I) - 1} \frac{a_{TF} d_p}{Z_i r_e m_e c^2} , \tag{17}$$

where I is the ionization potential ($I \simeq 172$ eV in Si), Z_i the electric charge of the channeled particle with its relativistic γ, while r_e and m_e are, respectively, the classical radius and rest mass of the electron. However, electronic dechanneling only describes a “slow" dechanneling regime, due to the very small variation in momentum from scattering with electrons in the channel, leading to an incomplete treatment of the whole process. Hard scattering on nuclei can lead to “fast" dechanneling as a result of single interactions. Therefore, a *characteristic nuclear dechanneling length* must also be taken into account for a reliable parameterization of the entire dechanneling process. This characteristic length for nuclear dechanneling can be derived by appropriate scaling of the electronic value, based on fine tuning using experimental data, as clarified in Section 3.2.1.

A solid theoretical analysis is needed to describe the probability that an incident particle will be captured in the crystal volume. This can be found in [17], where the dependence of such a probability is derived as a function of the particle energy E and crystal bending radius R, and can be written as:

$$P_{VC} = k \left(\frac{R}{R_c} - 0.7 \right) E^{0.2} , \tag{18}$$

where k is a constant tuned using comparisons between simulations and experimental data. When the particle is captured, it is treated as channeled and the possibility of a subsequent dechanneling interaction should be taken into account, as explained in Section 3.2.1.

2.4 Volume reflection

Particles that impinge on bent crystals with an incident angle in the range $\theta_c < \theta < \theta_b$, where θ_c and θ_b are the critical angle and bending angle of the crystal, can experience what is called *volume reflection* (VR). Protons that undergo this process are literally reflected by the interaction with the averaged potential of crystalline planes. In particular the reflection takes place when particles impinge on a crystalline plane with their momentum tangential to it. The extension of the angular range over which this tangency condition can be reached is determined by geometrical considerations only. It is clear that this condition can be achieved quite easily by particles entering bent crystals[2] with an angle slightly above the critical

[2] In direction of the bending.

one (where bounded states are no longer possible). If particles enter a bent crystal with an angle larger than the crystal bending, it will be impossible to reach a condition in which the momentum is parallel to the crystalline planes. An example is shown in Fig. 8.

Another key feature of the reflection process is how much the incident angle is modified, which is linked to the critical channeling angle in straight crystals. From simulation studies [18] it was possible to derive that, for crystals with $R \gg R_c$, the average deflection given to reflected protons is $\sim 1.6\theta c$. This has been experimentally proven in [19]. The dependence of such deflections as a function of the important crystal parameters was then derived. A good description [17] that fits experimental data for both the average deflection (θ_{VR}) and its spread($\Delta\theta_{VR}$), is:

$$\theta_{VR} = c_1\, \theta_c \left(1 - c_2 \frac{R_c}{R}\right) \tag{19}$$

$$\Delta\theta_{VR} = c_3\, \theta_c\, \frac{R_c}{R} \tag{20}$$

where c_1, c_2 and c_3 are empirical coefficients tuned to reproduce experimental data, as explained in section 3.2.1.

3 Simulation tools

In large accelerating machines such as the Large Hadron Collider (LHC), the prediction of how particle losses are distributed along the ring is crucial. This is mainly because superconducting magnets are used, and energy deposited in them could cause quenches that must be avoided at any time. A very complex multi-stage collimation system composed of about fifty collimators per beam is used at the LHC. To adequately evaluate losses of the order of 10^{-5}, statistics of 10^6–10^7 particles intercepted by the collimation system are needed. For the present system, these particles are tracked typically for 200 turns. It is easy to understand that the results of interactions with obstacles along the particle trajectories are a mandatory feature of any simulation tool that aims to carry out collimation studies. Therefore, it is clear that very fast simulation routines are crucial to describe interactions with collimator jaws, and to obtain results in a reasonable computing time.

In the case of studies on crystal-assisted collimation for the LHC, the requirement to have a very fast routine that describes the interaction of protons with a bent crystal is even more critical. This is because the system is designed to provide beam losses of the order of 10^{-6}, meaning that statistics of more than 10^7 protons intercepted by the crystal are needed. Also note that when a crystal of a few mm of silicon is acting as a scraper (i.e. the crystal is not oriented for optimal steering of halo particles by crystal channeling), particles have to be tracked for about 3000 turns before being absorbed by the collimation chain, mainly due to the small angular spread given by multiple Coulomb scattering. Protons must traverse such a misoriented crystal many times in order to accumulate a kick that is enough to reach the next collimation stage. Therefore, a crystal routine suitable for such complex and demanding simulations has to determine the interaction experienced by any proton based on just a few extractions of random numbers.

The standard tool used at CERN for collimation studies is based on the particle tracking code named `SixTrack` [3]. It is written in Fortran 77 and was originally developed to study non-linearities and the dynamic aperture in circular accelerators. Over the years it was modified in order to track large numbers of particles, also taking into account interactions with collimator jaws. This led to a collimation version of `SixTrack` [5,6,20], in which a routine that treats the interactions of protons with bent crystals was implemented. This code allow to estimate the density of proton lost per meter on the geometrical machine aperture along the entire ring, with a resolution of 10 cm.

3.1 The scattering routine

When a proton intercepts a collimator jaw along its path, a dedicated routine is called in `SixTrack` to simulate the interactions with matter. A description of the initial routine based on the `K2` code is given in [21]. This routine is regularly maintained. A detailed discussion of the physics models implemented, and the latest improvements, can be found in [22] and [23], respectively. This scattering routine is one of the key components for simulations of expected beam loss pattern around the entire accelerator, as a function of collimation settings and machine parameters. The benchmarking of simulated beam loss pattern in the LHC with respect to the measured one is reported in [24]. In this section only a list of the interactions treated is given. The same concepts and models have been implemented in the scattering routine used by the crystal routine described in section 3.2.

The interactions present in the scattering routine can be divided into two families: *nuclear point-like* and *continuous* interactions.

- **Continuous interactions**:
  - Multiple Coulomb scattering, where particles are stochastically scattered from components of matter.
  - Rutherford scattering, which takes place when particles have a small impact parameter on the material constituent leading to a larger scattering angle compared to Coulomb scattering.
  - Energy loss by ionization, i.e. the energy released to atomic electrons along the path inside the material.
- **Nuclear point-like interactions**:
  - Deep inelastic scattering, where the incident protons “disappear". The hadronic shower produced is not simulated and the proton is considered as absorbed in the collimator jaw at that spatial point.
  - Nuclear elastic scattering: protons emerge from the interaction with their momentum altered only in direction, but with a value that can be significantly larger than from Coulomb scattering.
  - Proton-proton and proton-neutron elastic scattering. The results of these interactions are the same as the previous item, but are in this case a consequence of the interaction with an atomic constituent.
  - Single-diffractive events, where protons emerge with their momentum only slightly altered in direction but significantly changed in magnitude.

3.2 The crystal routine

The crystal routine was originally developed as a stand-alone routine, written by Igor Yazynin in Fortran 77. It was then inserted in `SixTrack` by Valentina Previtali as part of her PhD work [25], where details of its implementation and issues of orientation with respect to the beam envelope can be found. The inclusion of possible crystal imperfections was also modeled, such as the presence of an amorphous layer and a miscut angle, further discussed in [25]. The amorphous material is described as a layer that surrounds the crystal bulk, with a thickness given as an input. When protons are incident on this layer, they are treated as traveling in an amorphous material. The miscut angle is modeled as an additional angle applied to protons incident on the crystal front-face, while reduced impact parameters are defined if protons enter the crystal body from the side facing the circulating beam. In this section a detailed description of the physics models present in the routine and their range of validity are discussed. The main body of the crystal routine is composed of three fundamental blocks:

- A routine for the treatment of coherent interactions in bent crystals.

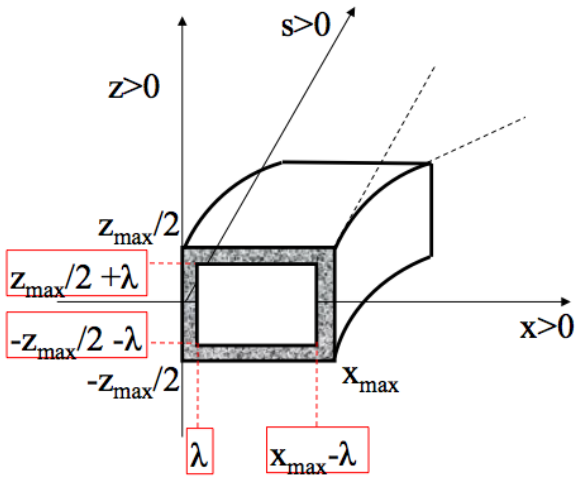

Fig. 9: Crystal routine reference system. The presence of a possible amorphous layer that surrounds the crystal bulk is also shown [25]

– A scattering routine, that treats the contributions of continuous and nuclear point-like interactions (see section 3.1).
– A routine that calculates the energy loss from ionization, described in [8].

3.2.1 Coherent interactions

The processes described in the routine are channeling for the whole crystal length, dechanneling, volume reflection, volume capture and dechanneling after volume capture. Inputs required by the routine, in the crystal reference system shown in Fig. 9, are:

– Crystal length (l) and bending radius (R).
– Momentum (p), and transverse coordinates (x) and (x') of the incident proton.
– The coordinates (z) and (z') are used only to evaluate if a proton is incident on a possible amorphous layer. Crystals are considered flat along this direction, which is an adequate approximation because of the very small dimensions of the beam compared to the crystal size (the usual crystal height is about 5 cm, whereas the beam halo has dimensions $\ll 1$ mm).

Using the quantities above it is possible to evaluate the critical channeling angle in straight (θ_c) and bent (θ_c^b) crystals together with the critical bending radius (R_c), using equations (5), (13) and (9) respectively. Then, the average deflection (θ_{VR}) and spread $(\Delta\theta_{VR})$ given by volume reflection are calculated together with the probability of volume capture (P_{VC}), using equations (19), (20) and (18) respectively. The free parameters used in these last three equations were tuned on experimental data taken in the framework of the H8-RD22 collaboration [19]. For strip crystals they are equal to:

$$c_1 = -1.5 \ , \ c_2 = 1.6667 \ , \ c_3 = \ 1.7 \ , \qquad (21)$$
$$k = 7 \cdot 10^{-4} \ .$$

For quasi-mosaic crystals c_1 is decreased by 7%, while c_3 is increased by 5%.

After calculation of all the parameters introduced above, a first selection based on incident angle is performed. It consists of checking that $\theta_{in} < \theta_c^b$, where θ_{in} is the linear sum of x' including a possible

miscut angle and crystal tilt with respect to the beam envelope. If this condition is satisfied the probability of capture between crystalline planes is calculated as follows:

$$P_{CH} = \frac{\sqrt{{\theta_c^b}^2 - {\theta_{in}}^2}}{\theta_c} \,. \tag{22}$$

This formula was derived to reproduce the channeling efficiency obtained with analytical simulation tools for a wide range of crystal parameters, i.e. length and bending, at a fixed energy. Using equation (13), if one assumes that a proton is incident with angle θ_{in} that is a fraction α of the critical value, thus:

$$\theta_{in} = \alpha\, \theta_c^b = \alpha\, \theta_c \left(1 - \frac{R_c}{R}\right) \,, \tag{23}$$

equation (22) can be expanded as follows:

$$P_{CH} = \left(1 - \frac{R_c}{R}\right) \sqrt{1 - \alpha^2} \,. \tag{24}$$

It is clear that equation (24) gives a $P_{CH} = 1$ in case of an incident beam with uniform divergence and optimal angle (i.e. $\alpha = 0$), on straight crystals (i.e. $R \to \infty$). This feature is not realistic, and such an approximation would be valid only if the protons were incident in the middle of the interplanar channel with transverse dimensions much less than the channel width. To allow the possibility for some incident protons to strike a crystalline plane, which precludes capture between two planes, equation (24) is replaced with:

$$P_{CH} = \left(1 - \frac{R_c}{R}\right) \sqrt{0.9 - 0.9\alpha^2} \,. \tag{25}$$

The maximum probability of capture between crystalline planes “saturates" at 95%. This value was adopted to fit experimental data for crystals with very small bending, as discussed in [8]. In particular, the difference between measured and simulated channeling efficiency was improved from about 10% to a few $\%$ for such crystals, while simulations of larger bending are not affected.

A random number with a uniform distribution in the range $[0, 1]$ is then generated, and if it is below the probability calculated using equation (25) protons are considered as initially trapped, otherwise they are flagged as being in the transition region between amorphous interactions and the volume reflection process. Then, for protons in this transition region, the deflection given is a linear interpolation between multiple Coulomb scattering (i.e. average deflection zero) and the expected value from the volume reflection process (i.e. θ_{VR} of equation 19). The incoming angle is modified as:

$$x' = x' + 0.45 \left(\frac{x'}{\theta_c^b} + 1\right) \theta_{VR} \,. \tag{26}$$

The spatial coordinates are moved to the middle of the path in the crystal volume, where the scattering routine is called to evaluate the contribution of amorphous interactions along the whole path. The five particle coordinates (p, x, x', y, y') are then propagated up to the exit from the crystal volume. The energy loss by ionization is also calculated for the whole path using a dedicated routine. This approach is denoted as the *thin lens approximation*: the full path in the amorphous material is divided into two steps, with the results of the interactions that take place applied at the mid-point and then used to propagate the proton coordinates as it leaves the volume. This approach is valid because the crystal dimensions (a few mm) are small compared to the radiation and interaction lengths (about 9 cm and 46 cm in silicon, respectively).

For protons that are considered trapped between crystalline planes the characteristic electronic dechanneling length is calculated. In bent crystals the equation (17) is modified as [1]:

$$L_D^e = \frac{256}{9\pi^2} \frac{pv}{\ln(2m_e c^2 \gamma / I) - 1} \frac{a_{TF} d_p}{Z_i r_e m_e c^2} \left(1 - \frac{R_c}{R}\right)^2 . \tag{27}$$

As explained in section 2.3 a characteristic nuclear dechanneling length is needed for full description of the dechanneling process. Unfortunately an analytical formula is not yet available in the literature. However, a characteristic length can be derived from an opportune scaling of the electronic value, and fine tuning was carried out to evaluate the best scaling constant, as explained in [26]. The characteristic nuclear dechanneling length is calculated in the routine as:

$$L_D^n = \frac{L_D^e}{200} . \tag{28}$$

This length is not calculated for all channeled protons but only a subset of them. The number of such protons is given by the ratio between the interplanar distance and the width of a crystalline plane. The width of a plane can be estimated using the Thomas-Fermi constant a_{TF}, while the interplanar distance for (110) silicon crystal planes is $d_p = 1.92$ Å [1]. Thus:

$$\frac{a_{TF}}{d_p} = \frac{0.8853 a_B Z^{-1/3}}{1.92} \approx \frac{0.194}{1.92} \approx 0.1 , \tag{29}$$

where $a_B = 0.529$ [1]. Thus, the nuclear dechanneling length is applied to only 10% of the protons initially channeled. Since the dechanneling process can be considered as an exponential decay of the initial population of trapped particles as a function of the distance travelled between crystalline planes, the possible point where dechanneling could take place is estimated as:

$$L = -L_D \ln(r) , \tag{30}$$

where L_D is the value calculated using either equation (27) or (28), and r is a uniform random number in the range $[0, 1]$. Thus, if L is smaller than the crystal length, the dechanneling process takes place at that depth in the crystal. Hence, protons are transported up to this point as channeled (described below), and then are propagated up to the exit from the crystal as traveling in an amorphous material, using the thin lens approximation. If L is larger than the crystal length, the proton is considered trapped between crystalline planes for the whole path in the crystal. The coordinates of the protons are modified as follows:

$$\begin{aligned} x' &= \frac{l}{R} + \frac{\theta_c^b}{2} r_g , \\ x &= x + l \sin\left(\frac{x'}{2} + m\right) , \\ y &= y + l\, y' , \end{aligned} \tag{31}$$

where m is the miscut angle and r_g is a random number with a normalized gaussian distribution. The energy loss from ionization is also calculated, together with the probability to experience nuclear interactions between crystalline planes as described later.

Let us move to protons incident with $\theta_{in} > \theta_c^b$. Initially the possible point where volume reflection could take place (l_{VR}), and its projection along s (s_{VR}), are evaluated as:

$$l_{VR} = R\,\theta_{in}\,, \tag{32}$$
$$s_{VR} = \sin\left(\frac{\theta_{in}}{2} + m\right) l_{VR}\,.$$

The possible reflection point l_{VR} is compared with the crystal length l. If $l_{VR} > l$ the volume reflection process cannot take place, and the proton is transported along its whole path in the crystal as in an amorphous material using the thin lens approximation. In the other case (i.e. $l_{VR} < l$) the probability of volume capture (P_{VC}) is calculated using equation (18). A uniform random number r in the $[0, 1]$ range is generated, and if $r > P_{VC}$ the proton is considered as reflected in the crystal volume. In this case, its coordinates are transported to the reflection point and the deflection given by the volume reflection process is applied. This is computed as:

$$x = x + x' s_{VR}\,, \tag{33}$$
$$y = y + y' s_{VR}\,,$$
$$x' = x' + \theta_{VR} + r_g\,\Delta\theta_{VR}\,.$$

The proton is transported along the path in the crystal as in an amorphous material using the thin lens approximation. If $r < P_{VC}$ the volume capture process takes place, and the coordinates (x, y) are transported to s_{VR} and a new dechanneling length is calculated. This length is based on an empirical model that fits experimental data taken in the framework of the H8-RD22 collaboration [27], and is equal to:

$$L_{VC} = L_D^e \left(\sqrt{0.01 - \ln(r)} - 0.1\right)^2\,. \tag{34}$$

Then this length is compared to the remaining path length in the crystal. If it is larger, the proton is considered captured between crystalline planes up to the end of its path, with consistent coordinate modifications. Otherwise, the proton undergoes dechanneling after the capture between planes. Then the proton is transported to the point of capture, then translated to the dechanneling point as for the channeling condition, and finally propagated up to the exit from the crystal using the thin lens approximation. Energy loss from ionization is calculated consistently for each different regime.

3.2.2 Scattering routine

The scattering routine is called when protons treated by the main crystal routine travel in amorphous silicon, as listed in the previous section. This routine includes the same physics models used in the standard routine of `SixTrack` to treat the interaction with collimator jaws, introduced in section 3.1. Thus, consistent modeling of nuclear point-like and continuous interactions with respect to standard CERN collimation tools is included in the crystal routine, maintaining the stand-alone nature of the routine.

The possibility to experience nuclear point-like interactions for particles trapped between crystalline planes is done by applying the scattering routine also during the path between crystalline planes, but considering only nuclear point-like interactions and using cross-sections scaled to the average nuclear density at the appropriate location. This is done in the assumption that the nuclear density between crystalline planes can be described as [1]:

$$\rho(x) = N_{am} \frac{d_p}{\sqrt{2\pi u_1^2}} \left[\exp\left(-\frac{x^2}{2u_1^2}\right) + \exp\left(-\frac{\left(x - d_p\right)^2}{2u_1^2}\right)\right]\,, \tag{35}$$

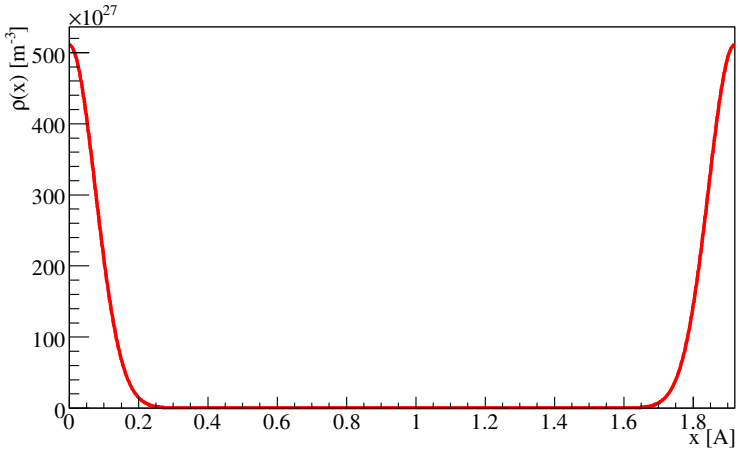

Fig. 10: Nuclear density between (110) planes of silicon, calculated with equation (35).

where x is the transverse distance from the crystalline planes placed at $x = 0$ and $x = d_p$, N_{am} is the density of misoriented silicon, and $u_1 = 0.075$ is the thermal vibration amplitude [1]. The nuclear density obtained using equation (35) is shown in Fig. 10. Using the equation of motion of protons between bent crystalline planes (equation (14)) it is possible to evaluate the maximum (x_M) and minimum (x_m) excursion from the equilibrium point, as:

$$x_m = -\frac{d_p}{2}\frac{R_c}{R} - \frac{d_p}{2}\sqrt{\frac{E_t}{U^b_{max}}}\,, \qquad (36)$$
$$x_M = -\frac{d_p}{2}\frac{R_c}{R} + \frac{d_p}{2}\sqrt{\frac{E_t}{U^b_{max}}}\,.$$

These two extremes oscillation amplitudes are calculated from the centre of the crystalline channel; a consistent shift of $-d_p/2$ must be applied to both of them in order to use the same reference frame as equation (35). Calculating the integral of equation (35) gives:

$$\int \rho(x)\,dx = N_{am}\frac{d_p}{2}\left[\mathrm{erf}\left(\frac{x}{\sqrt{2u_1^2}}\right) - \mathrm{erf}\left(\frac{d_p - x}{\sqrt{2u_1^2}}\right)\right]\,. \qquad (37)$$

The average density seen along the trajectory can be calculated analytically, as:

$$\bar{\rho} = \frac{\int_{x_m}^{x_M}\rho(x)\,dx}{x_M - x_m}\,. \qquad (38)$$

The equation above allows to avoid any numerical solution of complex integrals, maintaining the speed of the routine. What is obtained with this approximation is shown in Fig. 11. The average nuclear density seen by 400 GeV/c protons incident on a silicon strip crystal, 1.94 mm long and and with a 10.26 m bending radius, is plotted as a function of transverse energy. The detailed benchmarking with respect to experimental data of nuclear interaction rate in bent crystals is reported in [7, 8].

3.2.3 Limitations

It is crucial to have a clear understanding of possible limitations of any simulation routine in order to avoid those "working points". The weakness of the routine implemented in `SixTrack` is represented by

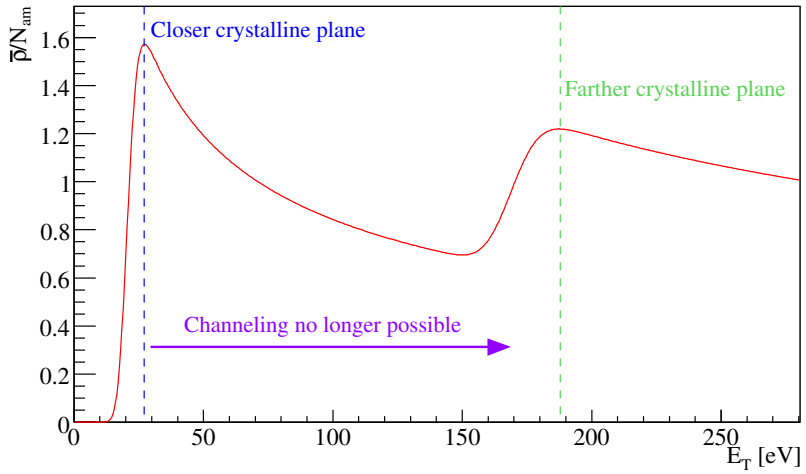

Fig. 11: Average nuclear density as a function of the transverse energy of 400 GeV/c protons, captured between (110) planes of silicon crystals 1.94 mm long and with a 10.26 m bending radius, as calculated using equation (38).

the description of nuclear dechanneling for extremely large bending angles. In these cases the potential well between crystalline planes is almost absent, and the few trapped particles are oscillating very close to the atoms. This condition is reached for a bending radius below three times the critical bending radius. An analytical treatment of such regimes is not yet available in the literature, and it could be reproduced only by simulation codes based on the integration of the equation of motion along the crystalline potential. Thus `SixTrack` simulations for crystals with $R < 3R_c$ cannot be fully reliable due to underestimated nuclear processes for such bending conditions.

4 Conclusions

The crystal routine and its implementation in `SixTrack` was described, together with the physics models used and their range of validity. This routine is suited for high statistics tracking simulations for beam loss pattern predictions in large hadron accelerators. The complete benchmarking of the crystal routine and of its implementation in `SixTrack` are reported in [7, 8]. The tools discussed allowed the design of a crystal collimation test stand in the LHC [8, 28] that led to the first observation of crystal channeling at the record energy of 6.5 TeV [29].

5 Acknowledgments

The authors would like to thank the LHC Collimation team in BE-ABP group, the UA9 Collaboration and the EN-STI group for the useful discussions and support during measurements.

References

[1] V. Biryukov, Y. Chesnokov, and K. V.I, *Crystal channeling and its application at high energy accelerators*. Springer, 1996.

[2] W. Scandale, G. Arduini, R. Assmann, F. Cerutti, S. Gilardoni, E. Laface, R. Losito, A. Masi, E. Metral, D. Mirarchi, *et al.*, "Strong reduction of the off-momentum halo in crystal assisted collimation of the SPS beam," *Physics Letters B*, vol. 714, no. 2, pp. 231–236, 2012.

[3] F. Schmidt, "SixTrack, User's Reference Manual," tech. rep., CERN SL/94-56 (AP), 1994.

[4] `http://sixtrack.web.cern.ch/SixTrack/`.

[5] G. Robert-Demolaize, R. Assmann, S. Redaelli, and F. Schmidt, "A new version of SixTrack with collimation and aperture interface," in *Particle Accelerator Conference, 2005. PAC 2005. Proceedings of the*, pp. 4084–4086, IEEE, 2005.

[6] `http://lhc-collimation-project.web.cern.ch/lhc-collimation-project/code-tracking-2012.php`.

[7] D. Mirarchi, G. Hall, S. Redaelli, and W. Scandale, "A crystal routine for collimation studies in circular proton accelerators," *Nuclear Instruments and Methods in Physics Research Section B: Beam Interactions with Materials and Atoms*, vol. 355, pp. 378–382, 2015.

[8] D. Mirarchi, *Crystal collimation for LHC*. PhD thesis, Imperial Coll., London , CERN-THESIS-2015-099, 2015.

[9] J. Stark *Phys. Zs.*, vol. 13, p. 973, 1912.

[10] V. Guidi, L. Lanzoni, and A. Mazzolari, "Study of anticlastic deformation in a silicon crystal for channeling experiments," *Journal of Applied Physics*, vol. 107, no. 11, p. 113534, 2010.

[11] S. Baricordi, V. Guidi, A. Mazzolari, D. Vincenzi, and M. Ferroni, "Shaping of silicon crystals for channelling experiments through anisotropic chemical etching," *Journal of Physics D: Applied Physics*, vol. 41, no. 24, p. 245501, 2008.

[12] A. Taratin, "Particle channeling in a bent crystal," *Physics of Particles and Nuclei*, vol. 29, no. 5, pp. 437–462, 1998.

[13] G. Moliére *Z. Naturforsch A*, vol. 2, p. 133, 1947.

[14] J. Lindhard and K. Dan *Vidensk. Selsk. Mat. Fys. Medd.*, vol. 34, p. 1, 1965.

[15] E. Tsyganov, "Preprints tm-682," *TM-684, Fermilab, Batavia*, 1976.

[16] Y. M. Ivanov, A. Petrunin, and V. V. Skorobogatov, "Observation of the elastic quasi-mosaicity effect in bent silicon single crystals," *Journal of Experimental and Theoretical Physics Letters*, vol. 81, no. 3, pp. 99–101, 2005.

[17] Y. A. Chesnokov, V. Maisheev, and I. Yazynin, "Volume capture and volume reflection of ultrarelativistic particles in bent single crystals," *arXiv preprint arXiv:0808.1486*, 2008.

[18] A. Taratin and W. Scandale, "Volume reflection of high-energy protons in short bent crystals," *Nuclear Instruments and Methods in Physics Research Section B: Beam Interactions with Materials and Atoms*, vol. 262, no. 2, pp. 340–347, 2007.

[19] W. Scandale, A. Vomiero, S. Baricordi, P. Dalpiaz, M. Fiorini, V. Guidi, A. Mazzolari, R. Milan, G. Della Mea, G. Ambrosi, *et al.*, "Volume reflection dependence of 400 GeV/c protons on the bent crystal curvature," *Physical review letters*, vol. 101, no. 23, p. 234801, 2008.

[20] R. Assmann, M. Brugger, M. Hayes, J. Jeanneret, F. Schmidt, I. Baichev, and D. KaItchev, "Tools for predicting cleaning efficiency in the LHC," in *Particle Accelerator Conference, 2003. PAC 2003. Proceedings of the*, vol. 5, pp. 3494–3496, IEEE, 2003.

[21] T. Trenkler and J. Jeanneret, "K2, a software package evaluating collimation systems in circular colliders (manual)," tech. rep., CERN-SL-Note-94-105-AP, 1994.

[22] N. Catalan-Lasheras, *Transverse and Longitudinal Beam Collimation in a High-Energy Proton Collider (LHC)*. PhD thesis, Zaragoza U., 1998.

[23] C. Tambasco, "An improved scattering routine for collimation tracking studies at LHC," Master's thesis, La Sapienza University of Rome, 2013.

[24] R. Bruce, R. Assmann, V. Boccone, C. Bracco, M. Brugger, M. Cauchi, F. Cerutti, D. Deboy, A. Ferrari, L. Lari, *et al.*, "Simulations and measurements of beam loss patterns at the CERN Large Hadron Collider," *Physical Review Special Topics-Accelerators and Beams*, vol. 17, no. 8, p. 081004, 2014.

[25] V. Previtali, *Performance evaluation of a crystal-enhanced collimation system for the LHC*. PhD thesis, EPFL These N.4794, CERN-THESIS-2010-133, 2010.

[26] D. Mirarchi, S. Redaelli, W. Scandale, A. Taratin, and I. Yazynin, "Improvements of the crystal routine for collimation studies," in *Proceedings of the International Particle Accelerator Conference*, p. 886, 2014.

[27] I. Yazynin *private communication.*

[28] D. Mirarchi, G. Hall, S. Redaelli, and W. Scandale, "Design and implementation of a crystal collimation test stand at the large hadron collider," *Eur. Phys. J. C*, vol. 77, p. 424, 2017.

[29] W. Scandale, G. Arduini, M. Butcher, F. Cerutti, M. Garattini, S. Gilardoni, A. Lechner, R. Losito, A. Masi, D. Mirarchi, *et al.*, "Observation of channeling for 6500 GeV/c protons in the crystal assisted collimation setup for LHC," *Physics Letters B*, vol. 758, pp. 129–133, 2016.